Analysis of seasonal and interannual variability in transpacific transport

Junfeng Liu and Denise L. Mauzerall
Woodrow Wilson School of Public and International Affairs, Princeton University, Princeton, New Jersey, USA

Larry W. Horowitz
Geophysical Fluid Dynamics Laboratory, Princeton, New Jersey, USA

Received 7 July 2004; revised 2 November 2004; accepted 30 November 2004; published 18 February 2005.

[1] The purpose of our analysis is both to evaluate the meteorological component of the seasonal and interannual variability of transpacific transport and to identify meteorological features that can be used to estimate transpacific transport. To accomplish this goal, we simulate the transport of nine continental tracers with uniform emissions and two-week lifetimes using the global Model of Ozone and Related Tracers Version 2 (MOZART-2) driven with NCEP reanalysis meteorology from 1991–2001. In addition, we define a transpacific "transport potential," a measure of the quantity of a tracer transported from a particular region normalized by its total emissions from that region, across a meridional plane in the eastern Pacific at 130°W. We find that at midlatitudes, the east Asian and Indian tracers have the largest transport potentials, particularly in spring. The interannual variability of the transpacific transport potentials of most tracers is relatively high in winter and fall (particularly in February and September) but is low from April to August. At high latitudes the former Soviet Union, east Asian, and European tracers have the largest transpacific transport potentials, especially in late summer and fall, when the lowest interannual variability is observed. We find that El Niño winters are associated with stronger eastward transport of east Asian emissions in the subtropical eastern Pacific. Transport of the east Asian tracer in the central North Pacific is well correlated with the North Pacific Index. However, we find that the interannual variability of transport across the west coast of North America is mostly driven by local meteorology. We therefore created a new index based on meteorology over the eastern Pacific, which we call the Eastern Pacific Index (EPI). The EPI captures most of the interannual variability of transpacific transport at both middle- and high-latitude regions across the west coast of North America.

Citation: Liu, J., D. L. Mauzerall, and L. W. Horowitz (2005), Analysis of seasonal and interannual variability in transpacific transport, *J. Geophys. Res.*, *110*, D04302, doi:10.1029/2004JD005207.

1. Introduction

[2] Transport of air pollutants across the North Pacific to North America has been identified by scientists [*Bailey et al.*, 2000; *Berntsen et al.*, 1999; *Jacob et al.*, 2003, 1999; *Jaffe et al.*, 1999; *Wilkening*, 2001] and is a growing concern to U.S. policy makers [*Carolina Environment Program* (*CEP*), 2004]. As Asia continues to industrialize, transpacific transport of pollution will increasingly affect air quality in the United States. Observations along the west coast of the United States and western Canada indicate that Asian anthropogenic emissions reach North America [*Jaffe et al.*, 1999, 2003; *Bailey et al.*, 2000]. Several major aircraft field campaigns, including PEM-West B (spring 1994), TRACE-P (February–April 2001), and ITCT (April–May 2002), have been conducted over the North Pacific in the past decade. Analysis of both observations and modeling simulations show that the processes associated with strong export of Asian emissions to the Pacific in spring include: (1) transport in the boundary layer behind cold fronts [*Liu et al.*, 2003], (2) vertical transport via convection, orographic lifting, frontal lifting and ascension in the warm conveyor belts (WCBs) of midlatitude storm tracks [*Heald et al.*, 2003; *Hess and Vukicevic*, 2003; *Liu et al.*, 2003; *Stohl et al.*, 2002; *Yienger et al.*, 2000], and (3) rapid transport in the lower free troposphere over the Pacific [*Bey et al.*, 2001; *Jacob et al.*, 2003; *Liu et al.*, 2003; *Stohl et al.*, 2002]. Transport of Asian emissions to the North Pacific is strong in spring, but weak in summer [*Balkanski et al.*, 1992; *Liu et al.*, 2003; *Wild and Akimoto*, 2001]. The maximum concentration of Asian pollutants is typically within the boundary layer, but the highest westerly outflow occurs in the middle troposphere [*Bey et al.*, 2001; *Liu et al.*, 2003]. Besides Asia, anthropogenic emissions from Europe and biomass burning in Africa also join the Asian outflow [*Bey*

0148-0227/05/2004JD005207$09.00

et al., 2001] and have been found to influence air quality over the Pacific and North America [*Fiore et al.*, 2002; *Jacob et al.*, 1999; *Lin et al.*, 2000; *Mauzerall et al.*, 2000].

[3] Most previous analyses have focused on mechanisms of export from the Asian continent and seasonal variations in transport, while only a few studies have examined the interannual variability in transport or the mechanisms for tracer transport across the Pacific. *Davis et al.* [2003] compared modeling results with observations from the PEM-WEST B and TRACE-P campaigns and found no significant systematic increasing trend in the concentration of any ozone precursors and no significant change in the level of photochemical activity over the western North Pacific between spring 1994 and 2001. *Liu et al.* [2003] compared the concentrations of Asian CO at 140°E in the springs of 1994, 1998, 2000 and 2001, and found that Asian outflow in the lower free troposphere was strongest in 1998 and in the upper troposphere was strongest in 2001. *Lamarque and Hess* [2004] found that the Arctic Oscillation can explain up to 50% of the springtime ozone variability in the lower troposphere over North America. We wish to examine the meteorologically driven component of interannual variability in transpacific transport as a first step in determining whether the influence of emissions from upwind continents is likely to have a relatively constant or highly variable effect on U.S. air quality.

[4] The major objectives of this paper are to identify the regions with the strongest geographic and meteorological potential to transport emissions across the North Pacific, to evaluate the meteorological component of the interannual variability of transpacific transport, and to identify the principal factors that drive this interannual variability. Variations in emissions (including magnitude, location and reactive species), photochemistry, and meteorology all contribute to the interannual variability of transpacific transport of air pollution. A follow-up study will examine the role that variability in emissions and chemistry has on transport. Here we focus exclusively on the influence of meteorology on transport. The methods we use are described in section 2. In section 3 and 4, we compare the transport pathways and timescales of Asian, European and African tracers using 11-year mean transport results. We use the "transport potential," the percentage of a tracer emitted from a region that is transported across a meridional plane downwind, to quantify and compare the seasonal and interannual variability of transpacific transport. The connections between the interannual variability of transpacific transport and both the El Niño-Southern Oscillation (ENSO) and the NPI are discussed in section 5. We introduce the EPI to describe the interannual variability in transport across the west coast of the United States (130°W) in section 6. Finally, conclusions are summarized in section 7.

2. Methods

[5] We use MOZART-2 (Model of Ozone and Related Tracers, version 2), a 3D global chemical tracer model [*Horowitz et al.*, 2003], driven with NCEP/NCAR reanalysis data [*Kalnay et al.*, 1996] to examine the variability in transpacific transport of chemical tracers between 1991 and 2001. MOZART is built on the framework of the Model of Atmospheric Transport and Chemistry (MATCH), which includes representations of advection, convective transport, boundary layer mixing, and dry and wet deposition. Advection of tracers is based on the flux-form semi-Lagrangian advection scheme [*Lin and Rood*, 1996], and convective flux transport is re-diagnosed using the *Hack* [1994] scheme for shallow and midlevel convection and the *Zhang and Mcfarlane* [1995] scheme for deep convection. A detailed description of MOZART-2 and evaluation of model results using climatological winds from the middle atmosphere community climate model, version 3 (MACCM3) with observations for ozone and its precursors is given by *Horowitz et al.* [2003]. In this work, we drive MOZART-2 with NCEP/NCAR assimilated meteorology at a horizontal resolution of approximately 1.9° latitude × 1.9° longitude with 28 sigma vertical levels from the surface to 2.7 mb. The NCEP/NCAR reanalysis data are converted from the original T62 resolution (with Gaussian latitudes) to a regular latitude grid by using spherical harmonic interpolation routines, and then smoothed by a 9-point local smoother. Meteorological parameters are provided to MOZART-2 every 6 hours. A 15 min time step for all transport processes is used.

[6] The simulation includes most transport processes (except dry deposition and wet scavenging) but holds tracer emissions and chemical lifetimes constant. The simulation covers the period from April 1990 to December 2001 with the first eight months used to initialize the simulation.

[7] Most previous studies treat Asia or part of Asia as an individual region [*Liu et al.*, 2003; *Stohl et al.*, 2002; *Wild and Akimoto*, 2001]. However, there are distinct emission and dynamical characteristics over the Asian continent. Thus we tagged tracer emissions from nine regions: besides North America (NA), South America (SA), Africa (AF), Europe (EU) and Australia (AU), we divided the Asian continent into east Asia (EA), southeast Asia (SE), India (IN) and the rest of Asia including the former Soviet Union (FSU) and the Middle East as shown in Figure 1. To obtain general information about transport features, we include only uniform tracer emissions from all nine continents at a rate of 10^{11} molecules cm^{-2} s^{-1}. Annual emissions of each tracer are listed in Table 1. These tracers do not represent chemical species, but are used to identify meteorological transport properties. Tracers with lifetimes of 2 and 4 weeks are emitted from each region. We use the 2-week lifetime tracers (long enough to be transported across the Pacific but short enough to have little likelihood of circling the earth) for the bulk of our analysis and use the 2 and 4 week lifetime tracers together to calculate transport timescales (section 3.2).

[8] We focus our analysis on the monthly mean transport of each tracer in order to examine the seasonal and interannual variability of transpacific transport. Therefore the analysis is more consistent with an evaluation of variation in background concentrations than an analysis of episodic transport. Our identification of transport pathways based on tracer fluxes differs from the approach of *Stohl et al.* [2002], who based their analysis on tracer concentrations.

3. Pathways and Timescales of Transpacific Transport

3.1. Transpacific Transport Pathways

[9] Transpacific transport is influenced by meteorology over both source regions and the North Pacific. Strong

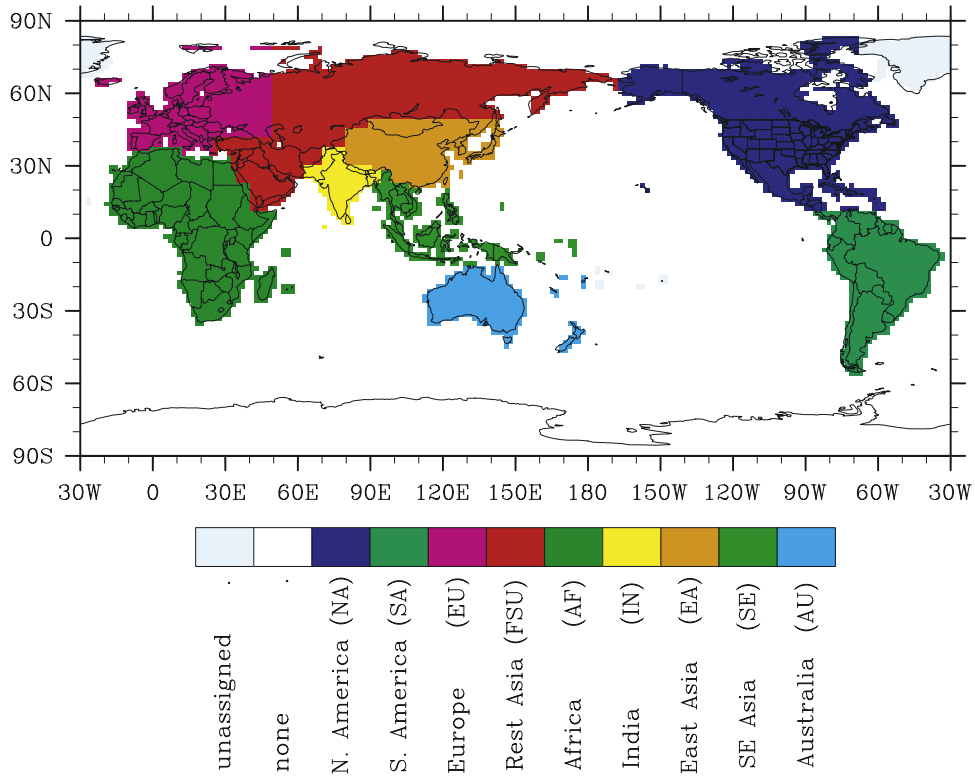

Figure 1. Tagged tracer emissions from nine regions.

seasonal variation occurs with maximum transport in winter and spring, and minimum transport in summer [*Bey et al.*, 2001; *Liu et al.*, 2003]. We therefore focus on transport in winter and spring. To illustrate the major transpacific pathways, we compare the mean December through April tracer fluxes that enter the western Pacific at 140°E (Figure 2) with the fluxes that leave the eastern Pacific at 130°W (Figure 3). We also show the horizontal distribution of total column tracer fluxes for the same period in Figure 4. Since we focus on the eastward transport of tracers across the North Pacific, we do not analyze the transport of North American, South American or Australian tracers.

[10] Figure 2 shows the major pathways for the outflow of six tracers entering the western Pacific (140°E) in the winter and early spring. Most tracers cross 140°E between 30°N and 50°N. As shown in Figure 2, the primary outflow of tracers emitted from regions at high latitudes (Europe, FSU, and east Asia to some degree) occur at low altitudes (below 500 mb) and include some outflow between 70°N and 90°N. Outflow of tracers from tropical regions (India, Southeast Asia and Africa) occur at higher altitudes (above 700 mb) and no northerly pathway exists. The mixture of tracers crossing 140°E (excluding NA, SA and AU tracers) is approximately 10% EU, 35% FSU, 11% AF, 7% IN, 29% EA, and 8% SE tracers. Patterns of inflow to North America across 130°W (Figure 3) follow a similar pattern to outflow although fluxes are lower due to tracer decay and more dispersed due to mixing during transport. At 130°W the fraction of tracers from east Asia and India increase, but from FSU and Africa decrease, with the mixture being 12% EU, 20% FSU, 5% AF, 19% IN, 34% EA, and 10% SE tracers.

[11] East Asian emissions occur at the latitude of most rapid eastward transport. Maximum outflow occurs between 25–50°N extending from the surface to about 400 mb, with a maximum at 40°N in the boundary layer. This transport pattern persists across the Pacific to the west coast of North America (Figure 4a) although the magnitude of tracer flux is reduced by a factor of 3 due to chemical decay and dilution (Figure 3a). The center of maximum flux at 130°W is still at 40°N, but due to elevation in warm conveyor belts (WCBs) in the North Pacific storm track and the faster transport at higher altitudes, is now near 500 mb. Moreover, due to influence of the Aleutian low, at 130°W the plume shifts northward and covers a broader area (from 20°N to 80°N) at 500 mb.

[12] The maximum eastward outflow of both FSU and European tracers at 140°E is near the surface (Figures 2b and 2c), as was reported by *Stohl et al.* [2002]. In these high-latitude regions, cold temperatures suppress convec-

Table 1. Annual Emission Rate for Tracers From the Nine Regions in This Study

Region	Tmol/year
NA	1.44
SA	1.09
EU	0.63
FSU	1.45
AF	1.81
IN	0.30
EA	0.67
SE	0.55
AU	0.55

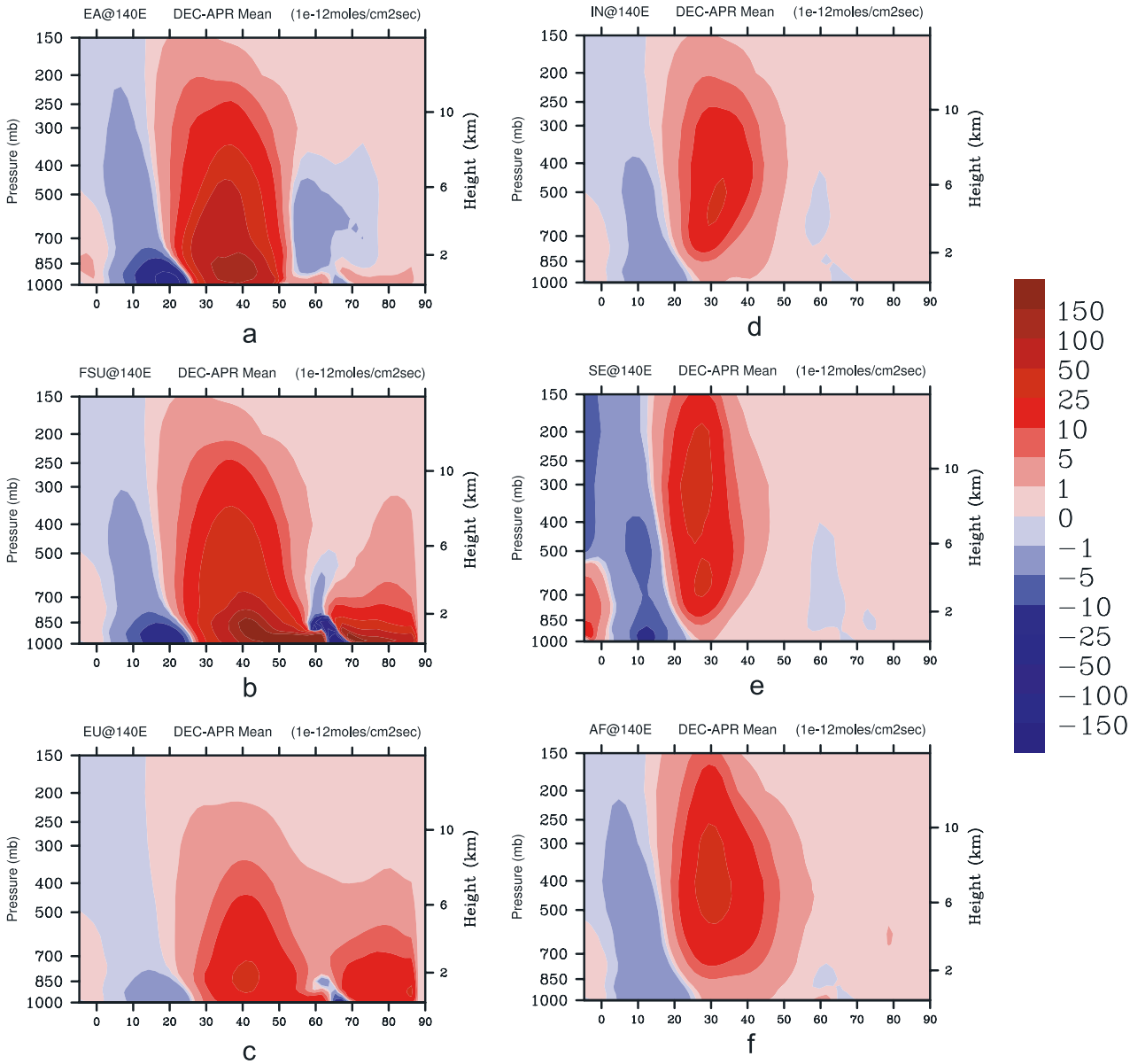

Figure 2. Vertical meridional cross sections over the western Pacific at 140°E of zonal tracer fluxes (in 10–12 mol/cm^2/s) averaged from December to April over 11 years (1991–2001) for tracers from (a) east Asia, (b) the former Soviet Union (FSU) and Middle East, (c) Europe, (d) India, (e) Southeast Asia, and (f) Africa. Positive fluxes are eastward.

tive activity during winter. The main outflow occurs at midlatitudes (30–60°N) similar to the east Asian outflow. A second pathway exists in the polar region (65–90°N) near the surface. This transport pattern persists across the Pacific, with the maximum flux remaining in the boundary layer at middle and high latitudes (Figures 3b and 3c). As shown in Figures 4b and 4c, the emissions from FSU and Europe first travel eastward at high latitudes (50–80°N), then split at approximately 120°E. Owing to the Siberian High over Mongolia and Siberia associated with strong southeastward cold fronts [*Bey et al.*, 2001], most tracer flow (EU: ~65%; FSU: ~80%) shifts southeastward and joins the midlatitude east Asian outflow. The remaining tracers north of 65°N shift northeastward at 120°E, cross the Arctic Ocean, and ultimately turn southeastward into central Canada and the eastern United States. The northern pathway is particularly important for the European tracer (Figure 4c) since it provides a short transport route from the source region across the Arctic to Canada and the northeastern United States.

[13] Tropical emissions (i.e., southeast Asia) are influenced by strong convection, which lofts tracers rapidly into the free troposphere and by the high altitude at which some tracers are released (i.e., India north of 25°N). The maximum eastward flux in winter and spring of the Indian tracer to the North Pacific occurs at 20–40°N and 300–700 mb (Figure 2d) with subsequent transport over the Pacific in the midlatitude westerlies (Figures 3d and 4d). North of 25°N, the Indian tracer is emitted between 850 and 650 mb, while emissions from southern India occur below 850 mb. Most

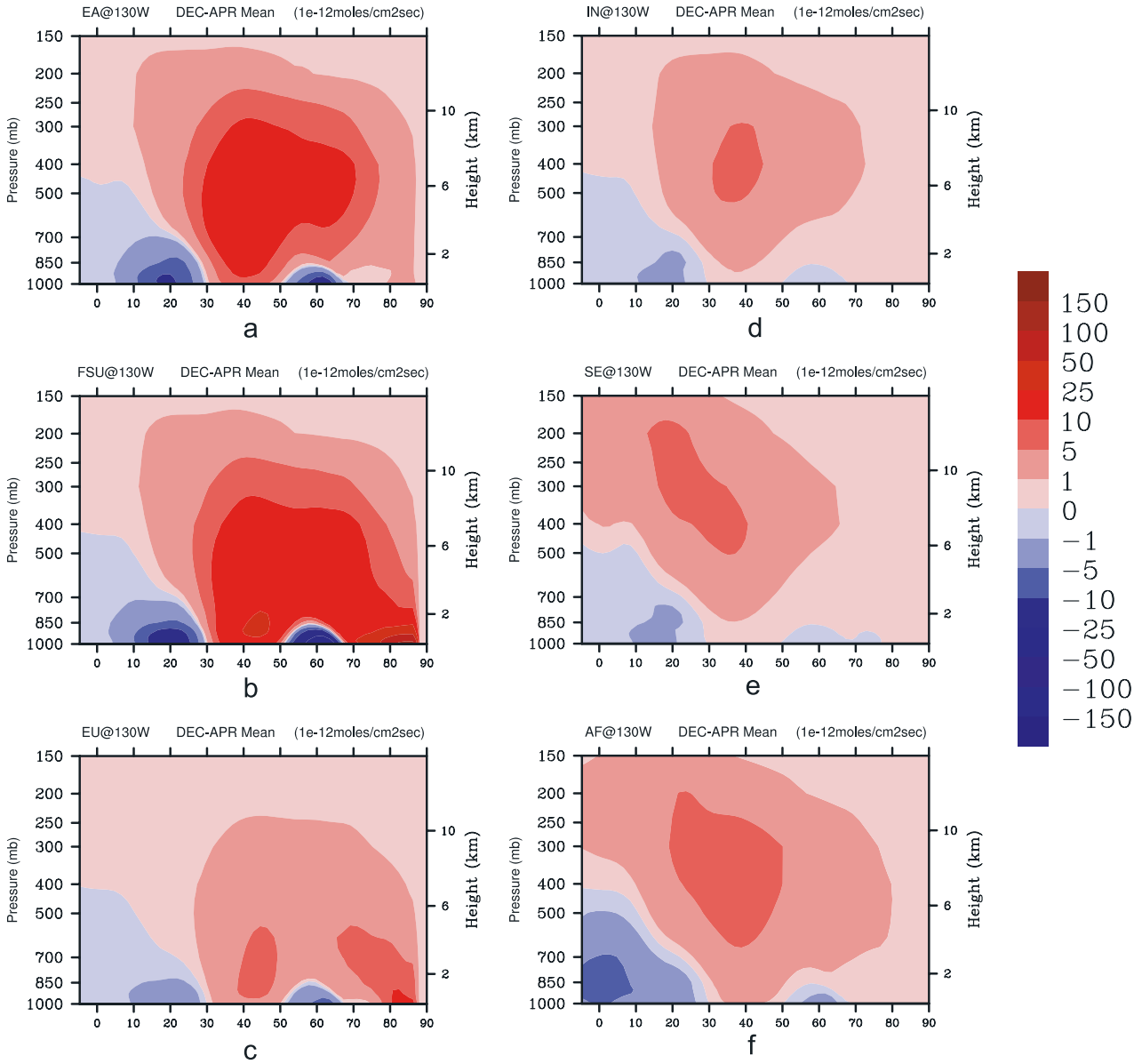

Figure 3. Same as Figure 2, but over the eastern North Pacific at 130°W.

emissions south of 20°N are captured by the tropical easterlies and travel west into the north Indian Ocean, a pattern observed by [*de Laat et al.*, 2001; *Verver et al.*, 2001]. This southern pathway persists in summer and brings summertime ozone produced from south Asian emissions into the Middle East [*Li et al.*, 2001]. Indian emissions north of 20°N merge with other tracers east of 100°E and are transported toward North America in the midlatitude westerlies (Figure 4d).

[14] Southeast Asian tracer is exported at low altitudes in the tropical easterlies toward the Indian Ocean and is also convected to high altitudes where it is transported in the midlatitude westerlies toward North America (Figures 2e, 3e, and 4e). Similarly, African emissions south of 20°N are primarily exported in the tropical easterlies toward the equatorial and South Atlantic Ocean while emissions north of 20°N are captured in the midlatitude westerlies and join the east Asian outflow across the North Pacific.

[15] Outflow over the North Pacific contains a mixture of emissions from a much broader region than just east Asia. However, we find that most emissions crossing the North Pacific are transported in the midlatitude westerlies.

3.2. Transpacific Transport Timescales

[16] By using isentropic back-trajectories to examine episodic events, *Jaffe et al.* [1999] estimated that pollution can be transported from east Asia to Cheeka Peak Observatory (CPO) in Washington State within 10 days. *Bailey et al.* [2000] also examined episodic events and estimated that 5 days were required for transport of east Asian emissions to western Canada. In addition, *Stohl et al.* [2002] used passive tracers to estimate that transpacific transport can occur in as little as one week. In this study, rather than focusing on episodic events, we estimate the average time required for transport from the emission source to any location downwind. We call the average time required for this transport

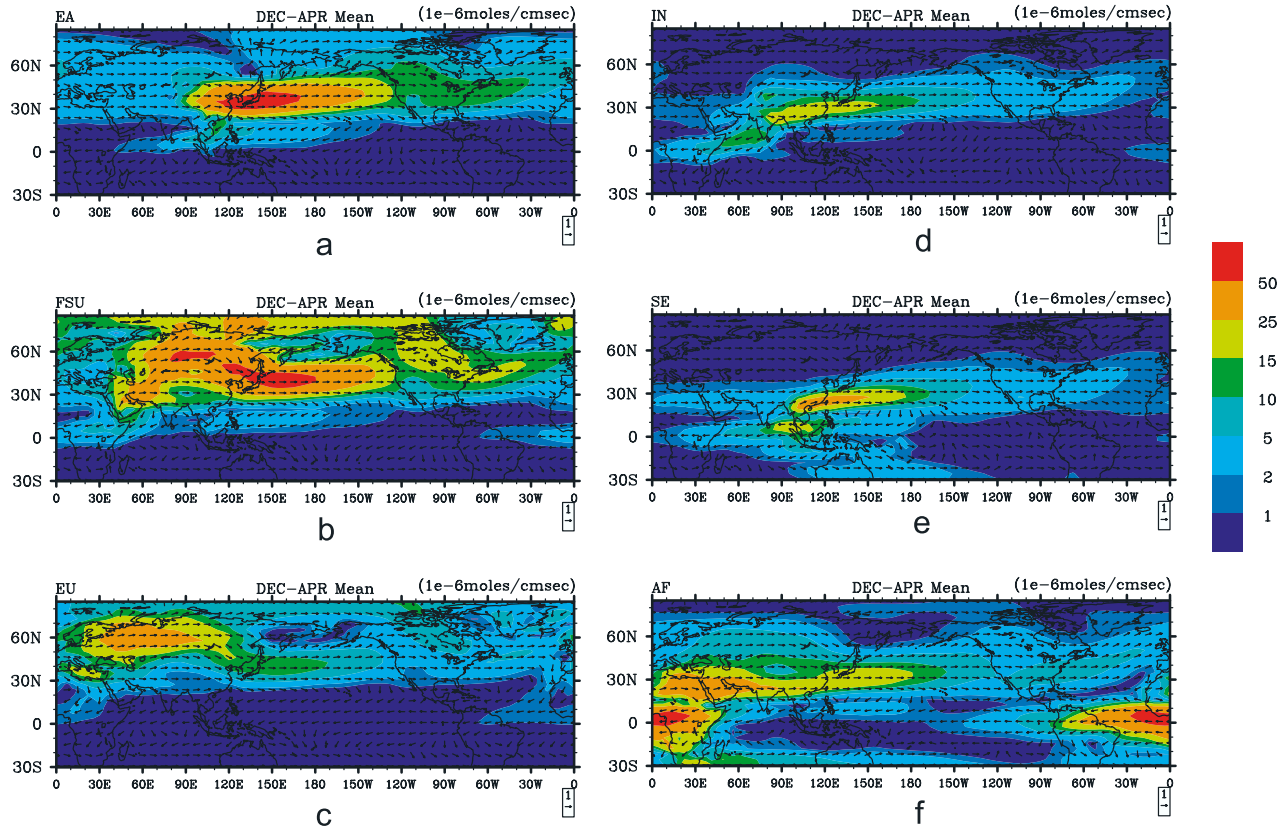

Figure 4. Horizontal distributions of total column tracer fluxes (in 10^{-6} mol/cm/s) between surface and 200 mb from December to April in the period 1991–2001 of tracers from (a) east Asia, (b) the former Soviet Union (FSU) and Middle East, (c) Europe, (d) India, (e) Southeast Asia, and (f) Africa. (Arrows indicate flux direction, and gray scale represents flux magnitude.)

the "transport timescale." A similar "chemical clock" approach has been used to diagnose the age of pollution plumes [*Mauzerall et al.*, 1998; *McKeen and Liu*, 1993]. A detailed description of our method is in the work of J. Liu and D. Mauzerall (Average intercontinental transport timescales, submitted to *Geophysical Research Letters*, 2005); here we provide an overview.

[17] Our method assumes that the transport timescale can be represented by a ratio of the concentration of two tracers if the difference in the concentrations is only the result of a difference in tracer lifetimes. For two tracers with identical emission rates, the transport timescale can then be calculated by:

$$\Delta t = \frac{\tau_a \tau_b}{\tau_a - \tau_b} \ln\left(\frac{c_a}{c_b}\right), \qquad (1)$$

where τ_a and τ_b are the lifetimes of the two tracers a and b ($\tau_a \neq \tau_b$); and c_a and c_b are the concentrations of the two tracers at a particular location D. Δt is the transport time from the emission source to D.

[18] As indicated by *McKeen et al.* [1996], the "chemical clock" method is appropriate when applied to emissions from an isolated source if emissions and multiple sources are not considered. In our analysis, we use averaged multiyear seasonal data to calculate a mean transport timescale. Transport timescales strongly depend on tracer lifetimes when two or more major transport pathways to the same destination exist. The transport timescales obtained with equation (1) depend on the lifetimes of the tracers used.

[19] We focus on spring, the season of maximum transport. Figure 5 shows the horizontal distribution of tracer fluxes and the mean transport timescale for each tracer in spring at both the surface and at 500 mb (sigma level). Generally, the fastest transpacific pathway is associated with the largest transport. For the east Asia region, transpacific transport at the surface is approximately 1 week slower than transport at 500 mb due to frontal and convective lifting rapidly conveying tracers to the free troposphere and the strong midlatitudes westerlies. The FSU region is relatively cold, making vertical transport slow. The surface transport of FSU emissions into the Arctic Circle is very efficient compared to other regions, due to the high latitude of the source and limited vertical transport. At 500 mb, the FSU tracer is transported in the midlatitudes, but takes about one week longer than east Asian emissions to reach North America. European emissions are concentrated at high latitudes and far from the Pacific, thus the transpacific transport timescale is longer, requiring 4–6 weeks at the surface and 4–5 weeks at 500 mb to cross the Pacific. However, due to rapid transport across the Arctic, European tracers arrive more quickly in the northeastern United States (3–5 weeks) than in the

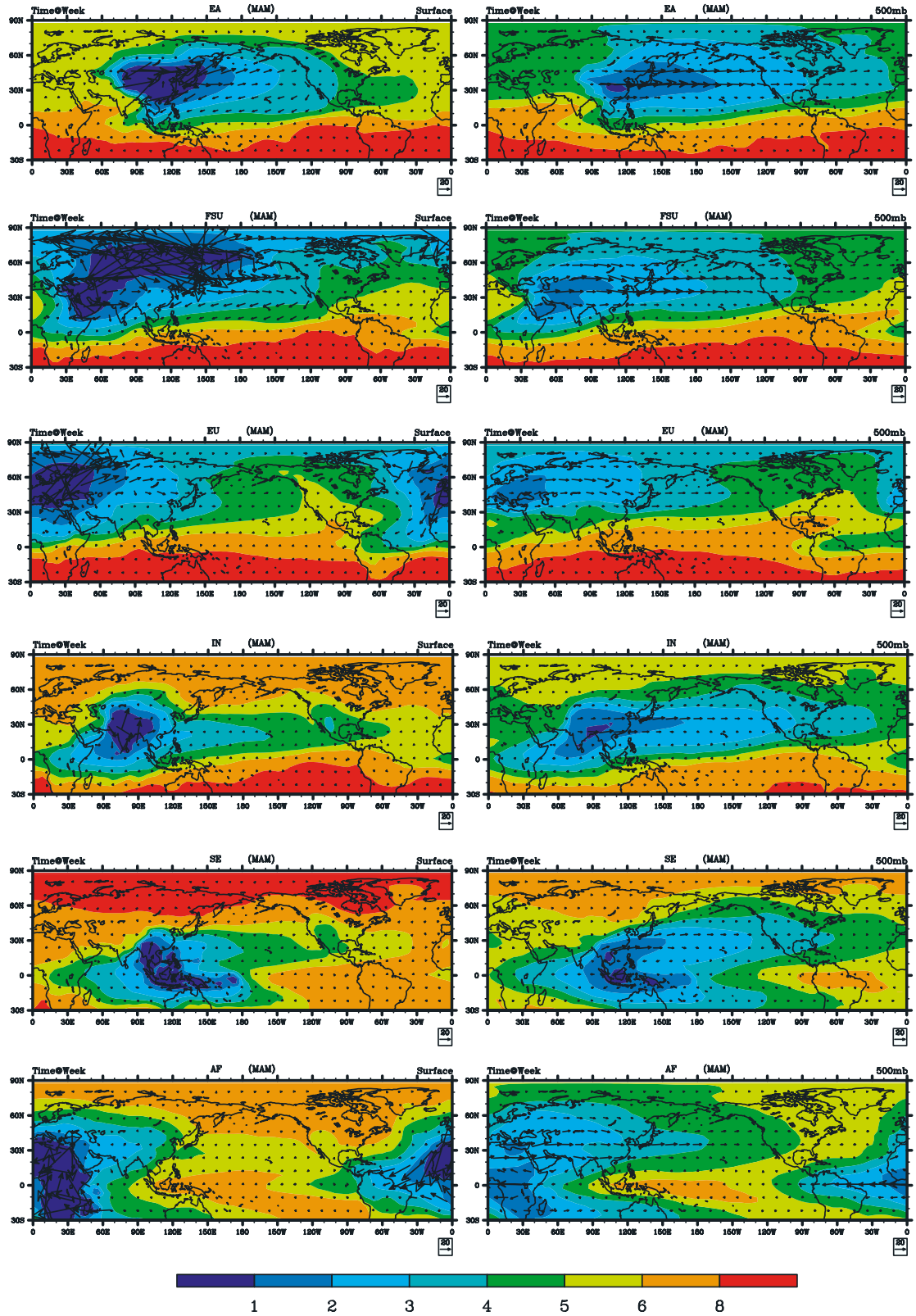

Figure 5. The 11-year (1991–2001) seasonal average transport timescales (unit: weeks) in spring (MAM) of tracers from east Asia, the former Soviet Union and Middle East, Europe, India, Southeast Asia, and Africa at surface (left column) approximately 500 mb (sigma level, right column). Arrows represent horizontal tracer flux (unit: 10^{-12} mol/cm^2/s).

western United States (5–6 weeks). Transpacific transport of the Indian tracer at 500 mb is very fast in spring, with a timescale similar to that of the east Asian tracer, but surface transport is much slower. Similarly, the southeast Asian tracer is transported much faster at 500 mb than at the surface. As the location is far from the Pacific, transport of the African tracer to North America takes much longer than tracers from other regions at both the surface and at 500 mb.

4. Transpacific Transport Potential

[20] To quantify and compare the transpacific transport of each region's emissions in a way that is not biased by the difference in total emissions from each region (resulting from their difference in size), we define a "transport potential" (equation (2)). The transport potential, α, is the percentage of a tracer emitted from a region ***S*** that is transported across a meridional plane ***D*** in the eastern Pacific, and is intended to reflect just the meteorological transport properties between ***S*** and ***D***. The transport potential is defined in equation (2):

$$\alpha(t_1, t_2, \tau) = \frac{F(t_2)}{E(t_1)} \times 100\%, \qquad (t_1 < t_2) \tag{2}$$

where $E(t_1)$ is the total average emission rate of the tracer at time 1, and $F(t_2)$ is the net eastward flux across a vertical-meridional plane at time 2. The difference between t_1 and t_2 represents the average transport timescale. However, the transport timescale varies depending on the tracer lifetime τ. The transport potential for a tracer with lifetime τ', $\alpha(t_1, t_2, \tau')$, can be approximated by the following equation if we know the transport potential for the tracer with lifetime τ, $\alpha(t_1, t_2, \tau)$:

$$\alpha(t_1, t_2, \tau') = \alpha(t_1, t_2, \tau) \cdot \exp\left[\left(\frac{\tau' - \tau}{\tau'\tau}\right)\Delta t_{21}\right], \tag{3}$$

where Δt_{21} is the average transport time from ***S*** to ***D***.

[21] We evaluate the transport potential (τ = 2 weeks) across meridional planes in the eastern Pacific at 130°W, near the west coast of North America, as defined in Figure 6. Figure 7 compares the seasonal and interannual variability of transpacific transport of the regional tracers by using the 11-year monthly mean and monthly relative standard deviation (RSD) (i.e., the ratio of the standard deviation of a monthly mean to the 11-year averaged monthly mean) of the transport potential (τ = 2 weeks) across each plane at 130°W.

[22] The seasonal variations of the transport potential of most tracers across the midlatitude plane at 130°W are strongest in spring and weakest in summer. However, this pattern does not persist at high latitudes, where the transport potential of certain tracers (i.e., FSU, EU, and EA) in late summer or fall is equal to or higher than in spring, probably due to the northward shift of the midlatitude Pacific jet stream in summer. The transport potential magnitudes reflect both the distance and meteorological conditions between source and destination. Owing to the strong midlatitude westerlies and tropical easterlies as well as the relative geographic positions, tracers emitted at middle- and high-latitude regions (i.e., EA, FSU, EU, IN) generally have higher transport potentials than tracers emitted in the tropics (i.e., SE and AF). Similarly, the transport potential for most tracers is significantly higher at middle or high latitudes than in the subtropics. In particular, the east Asian tracer has the highest transport potential at both middle and high latitudes (except in summer at high latitudes, where the FSU tracer ranks first). FSU and European tracers are emitted further north and rank second in high-latitude transport potential. Thus strong potential exists in summer for transport of emissions from Siberian fires to the high latitudes of North America, consistent with the findings of *Jaffe et al.* [2004]. The Indian tracer is transported efficiently in the midlatitude Pacific (particularly in spring), and ranks second in springtime midlatitude transport potential. The transport potentials of tropical emissions (i.e., the southeast Asian and African tracers) are generally very small.

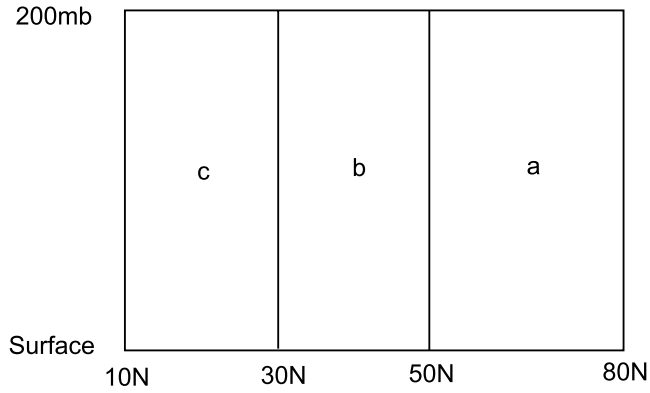

Figure 6. Vertical meridional planes used to calculate transport potentials at 130°W (off the west coast of North America). Planes extend from the surface to 200 mb with meridional extent (a) high-latitude plane (50–80°N), (b) midlatitude plane (30–50°N), and (c) subtropical plane (10–30°N).

[23] The RSD is used to evaluate the interannual variability of the transpacific transport potential. At midlatitudes, the RSD for most tracers is relatively high in winter and fall, particularly in February (RSD ~0.3–0.5) and September (RSD ~0.25–0.4), but low from April to August (RSD: ~0.15–0.3). The east Asian tracer has the lowest RSD (~0.3 in February; ~0.15 in April and July) throughout the year, indicating that its transport is generally more stable than other tracers. The transport of European and FSU tracers is stable in April (RSD: ~0.15–0.17), but highly variable in February (RSD: ~0.5) and September (RSD: ~0.4). At high latitudes, RSD values are generally high in winter and spring (RSD: ~0.3–0.7) but low in summer and early fall (RSD: ~0.15–0.4). In the subtropics, the RSD values are sometimes very large (RSD > 2) due to both a small 11-year mean transport potential and relatively high transport variability.

[24] The seasonal and interannual variability of transport potentials indicates that April is the month of strongest midlatitude transport and low interannual variability in transport determined by meteorology (especially for east Asian emissions). Thus long-term measurements over the

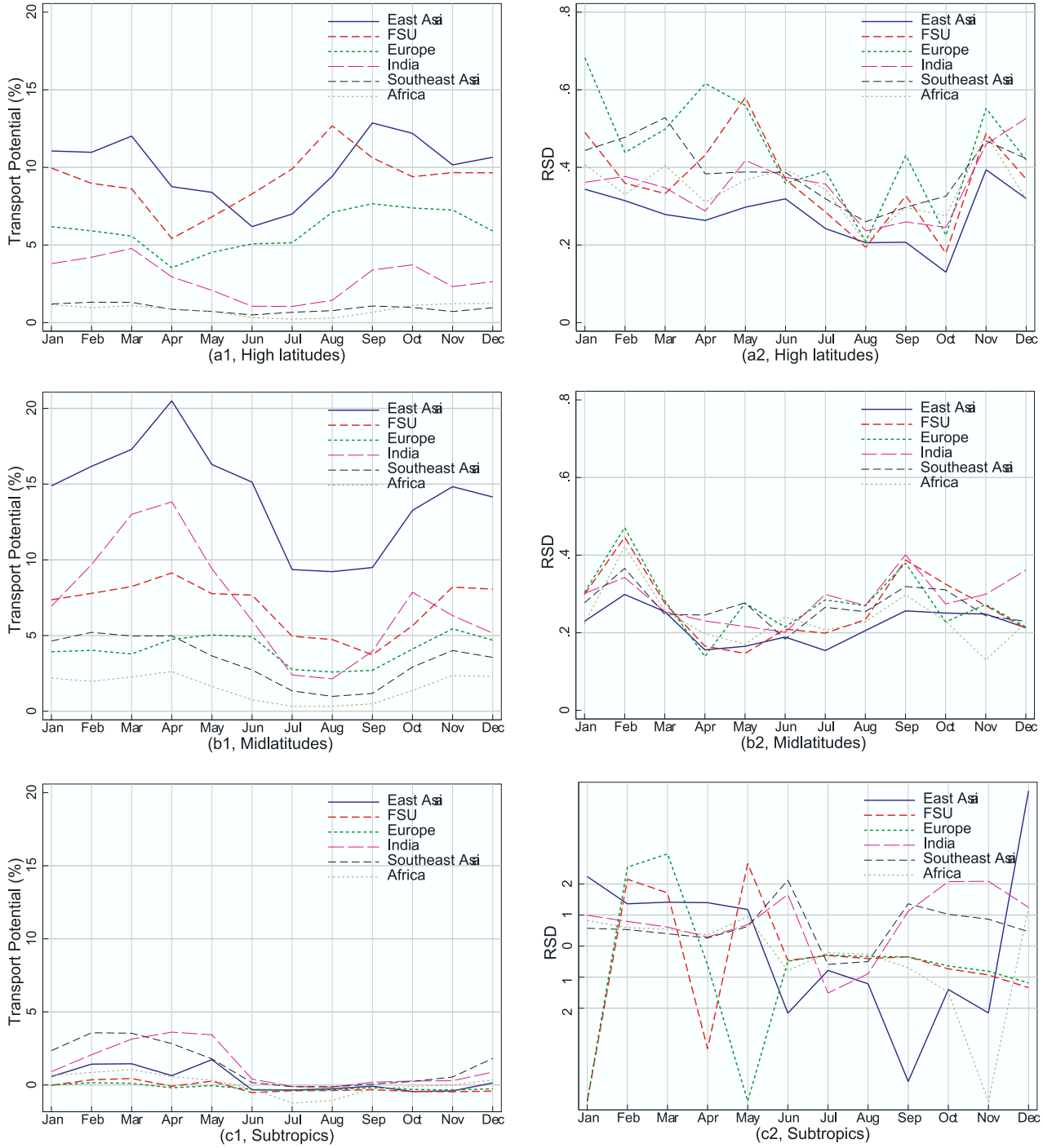

Figure 7. The 11-year (1991–2001) averaged monthly mean (left column) and relative standard deviations (ratio of the standard deviation of the monthly means to the 11-year monthly mean, right column) of transport potentials of tagged tracers across (top) the high-latitude plane (50–80°N), (middle) midlatitude plane (30–50°N), and (bottom) subtropical plane (10–30°N) at 130°W. (For the subtropical plane the RSD values have been limited to $-5 \leq \text{RSD} \leq 5$.)

western United States in April would reflect the interannual variability of emissions and chemistry more than other months. Midlatitude transport potentials in February are high for most tracers. However, the highest midlatitude RSD values in February suggest that interannual variability in meteorology determined transport is large in February (particular for FSU and European tracers). The transport potentials of FSU, east Asian and European tracers at high latitudes in late summer and fall are also large, but with relatively low RSD values indicating little variability in transport. Most studies, including surface measurements and aircraft campaigns, have focused on

spring transport. In the future, additional investigation of midlatitude transpacific transport in February and high-latitude transport in late summer and fall would be worthwhile.

5. Meteorological Factors Driving Interannual Variability

[25] In order to explain the meteorological component of interannual variability in transpacific transport we examine two major atmospheric indices, the SOI and the NPI. These indices capture large-scale dynamical features of transport over the Pacific in a simplified fashion. In this section, we evaluate the ability of these indices to explain variability in transpacific transport.

5.1. El Niño-Southern Oscillation (ENSO)

[26] The El Niño-Southern Oscillation (ENSO) is a well known source of interannual meteorological variability [*Orlanski*, 2003; *Philander and Fedorov*, 2003]. The SOI is calculated to monitor the ENSO phenomenon. SOI is defined as the difference between the sea level pressure anomalies at Tahiti and Darwin, Australia (Tahiti minus Darwin) [*Trenberth*, 1984]. Negative SOI values indicate El Nino conditions. Several studies indicate connections exist between ENSO and other meteorology which facilitates export of Asian emissions. For example, a strong correlation was found between a weak (strong) Siberian high which would decrease (increase) export and El Niño (La Nina) periods [*Zhang et al.*, 1997]. Moreover, *Liu et al.* [2003] found that the frequency of cold fronts over east Asia, the major process driving Asian pollution outflow in spring, was low in 1998 (El Niño) spring, but high in 2001 (La Niña) spring. However, no studies of which we are aware describe the detailed connections between ENSO and transport over the entire North Pacific. In this study, we evaluate the influence of ENSO on transpacific transport by correlating the transpacific transport potential anomalies (i.e., the transport potential for a particular month and tracer minus the 11-year mean transport potential for the same month and tracer) with the SOI values. The source of SOI values are from *Trenberth* [1984].

[27] The El Nino signal is strongest in winter. A strengthening and southward shift of the jet stream axis over the eastern North Pacific occurs during El Nino winters [*Orlanski*, 2003] suggesting that stronger eastward transport in the subtropics is possible. To examine the influence of SOI on transpacific transport, time series of monthly mean SOI and the monthly mean transport potential anomalies in winter of tagged tracers across the subtropical, midlatitude and high-latitude planes are shown in Figure 8. We find that transport and SOI are poorly correlated at middle and high latitudes (Figures 8a and 8b). However, strong anticorrelations exist in the subtropics (Figure 8c) confirming that more tracer is transported across the subtropical North Pacific during El Niño winters. The correlation coefficients in Table 2 indicate that ENSO influences the subtropical transport of tropical emissions (i.e., southeast Asia, Africa) more than the middle- and high-latitude emissions (i.e., India, east Asia, FSU and Europe) in winter. This trend persists (but is weaker) in spring and tends to reverse (i.e., ENSO influences the transport of middle- and high-latitude emissions more than that of tropical emissions) in autumn. The weakest correlations are found in summer indicating ENSO has little influence on summer transport.

[28] To further investigate the influence of ENSO on transpacific transport at 130°W, we plot the regressions of the monthly transport potential anomalies with the monthly SOI across the meridional plane at 130°W between December and April for six tracers (Figure 9). A strong regression signal reflects both a high correlation and large variation in transport, and can be used to identify regions influenced by ENSO. In winter and early spring, relatively strong eastward transport occurs around 30°N during El Niño, and around 50°N and in the tropics during La Niña. However, the magnitudes of the regressions depend on the transport pathway of the tracer. For example, SOI has a strong influence on tropical convection with weaker (stronger) convection occurring over southeast Asia during El Nino (La Nina) periods. Thus, since export of Southeast Asian emissions to the east occurs in high altitude westerlies, El Nino periods result in decreased export [*Liu et al.*, 2003]. To investigate the ENSO influence over the entire North Pacific rather than just at130°W, we plot the correlation coefficients between monthly SOI and the zonal column flux (from the surface to near 200 mb) of the east Asian tracer in winter and spring. A strong dipole pattern, which nearly disappears in other seasons, is found over the subtropical eastern Pacific. This pattern further confirms that the strongest ENSO influence on the transport of east Asian tracers to North America is in winter in the subtropical eastern Pacific (the region east of Hawaii).

5.2. North Pacific Index

[29] The North Pacific Index is defined as the area-weighted mean sea level pressure over the region 30° to 65°N, and 160°E to 140°W. Lower NPI values indicate a deepening and eastward shift of the Aleutian low pressure system, which brings warmer and moister air to the west coast of North America and Alaska and colder air to the central North Pacific [*Trenberth and Hurrell*, 1994]. The change of the position and intensity of the Aleutian low influences the atmospheric circulation at middle and high latitudes over the Pacific and might be expected to alter the pathway and intensity of transpacific transport.

[30] Because the Aleutian low is deepest in winter [*Trenberth and Hurrell*, 1994], we compare the NPI and monthly transport potential anomalies between December and February over the period 1991–2001. As shown in Figure 10, midlatitude transport is occasionally anticorrelated with NPI anomalies with a lower NPI frequently associated with higher transpacific transport. No correlation is observed for the transport in the subtropics, high-latitude regions or the total Northern Hemisphere for most of the tracers. As indicated in Table 3, extratropical transport (30°N–80°N) is only enhanced (decreased) for the Indian and Southeast Asian tracers when the NPI is anomalously low (high) in spring. The correlation patterns are weak for the east Asian, European and African tracers

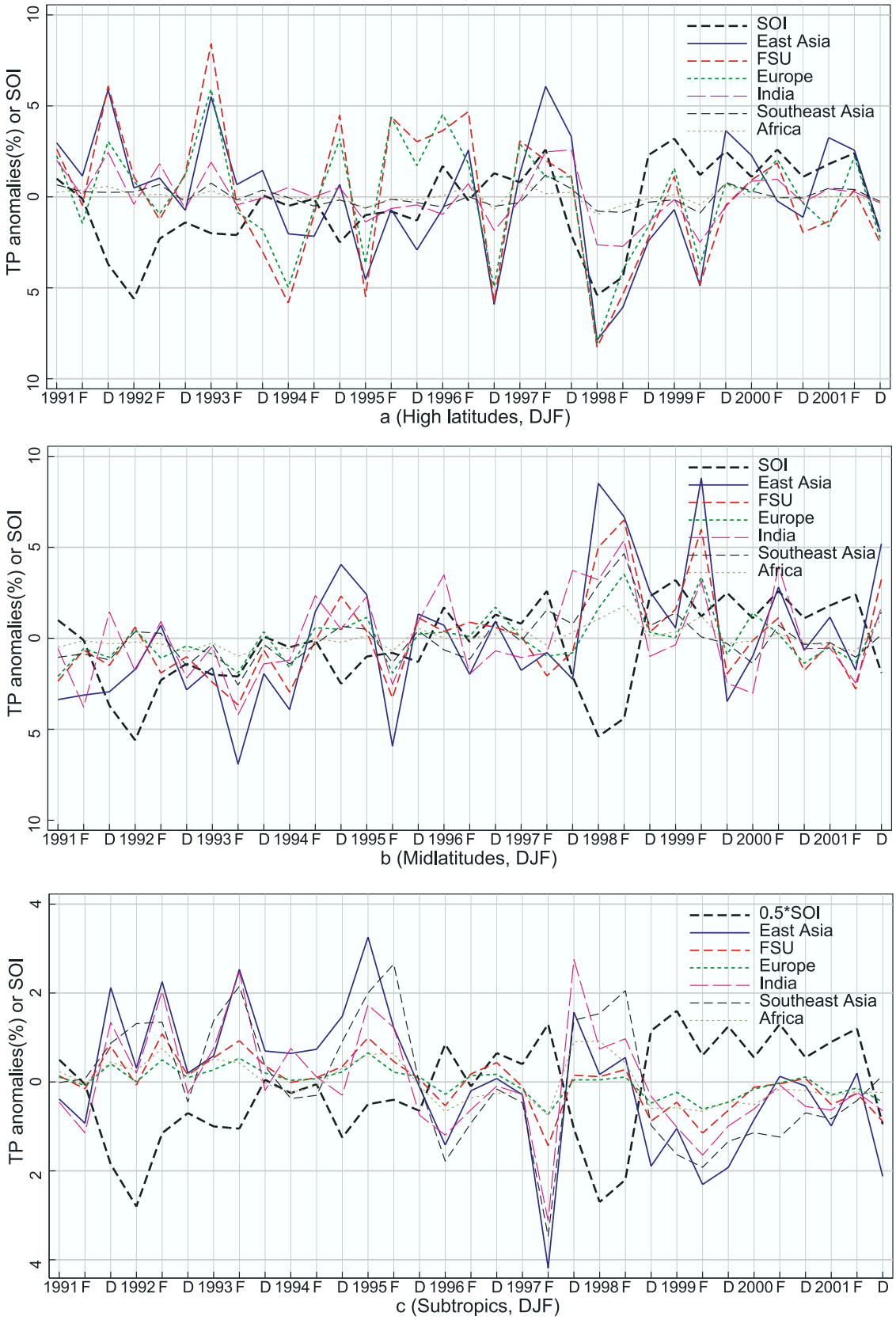

Figure 8. Time series of monthly mean SOI and monthly mean transport potential anomalies of tagged tracers across (a) high-latitude plane (50–80°N), (b) midlatitude plane (30–50°N), and (c) subtropical plane (10–30°N) at 130°W in winter (DJF). Negative SOI values indicate El Niño periods. Note the differences in scales and that the SOI index is multiplied by 0.5 in Figure 8c.

Table 2. Correlation Coefficients Between Monthly SOI and Monthly Subtropical Transport Potential Anomalies (10°N–30°N) at 130°W in Each Season (1991–2001)

Region	DJF	MAM	JJA	SON
EA	−0.55	−0.32	−0.06	−0.49
FSU	−0.53	−0.29	−0.23	−0.47
EU	−0.53	−0.33	−0.17	−0.43
IN	−0.59	−0.44	0.01	−0.50
SE	−0.77	−0.51	−0.10	−0.24
AF	−0.77	−0.59	0.15	−0.03

because the NPI is strongly anticorrelated with tracer transport in the central North Pacific (Figure 11b) rather than eastern North Pacific. A deeper Aleutian low (i.e., a lower NPI) is strongly correlated with stronger eastward transport at midlatitudes, but weaker eastward transport in the subtropics and high latitudes over the central North Pacific.

6. Development of the Eastern Pacific Index

[31] East Asian emissions are most likely, for both geographical and meteorological reasons, to be transported over the Pacific. In section 5, we found that neither the SOI nor the NPI are able to explain the interannual variability of transpacific transport potentials over the eastern Pacific, especially at middle and high latitudes where transport is strong. We defined the "transpacific transport potential" as the transport across 130°W in the eastern Pacific (Section 4), and found the main transport pathway of east Asian tracer to be in the

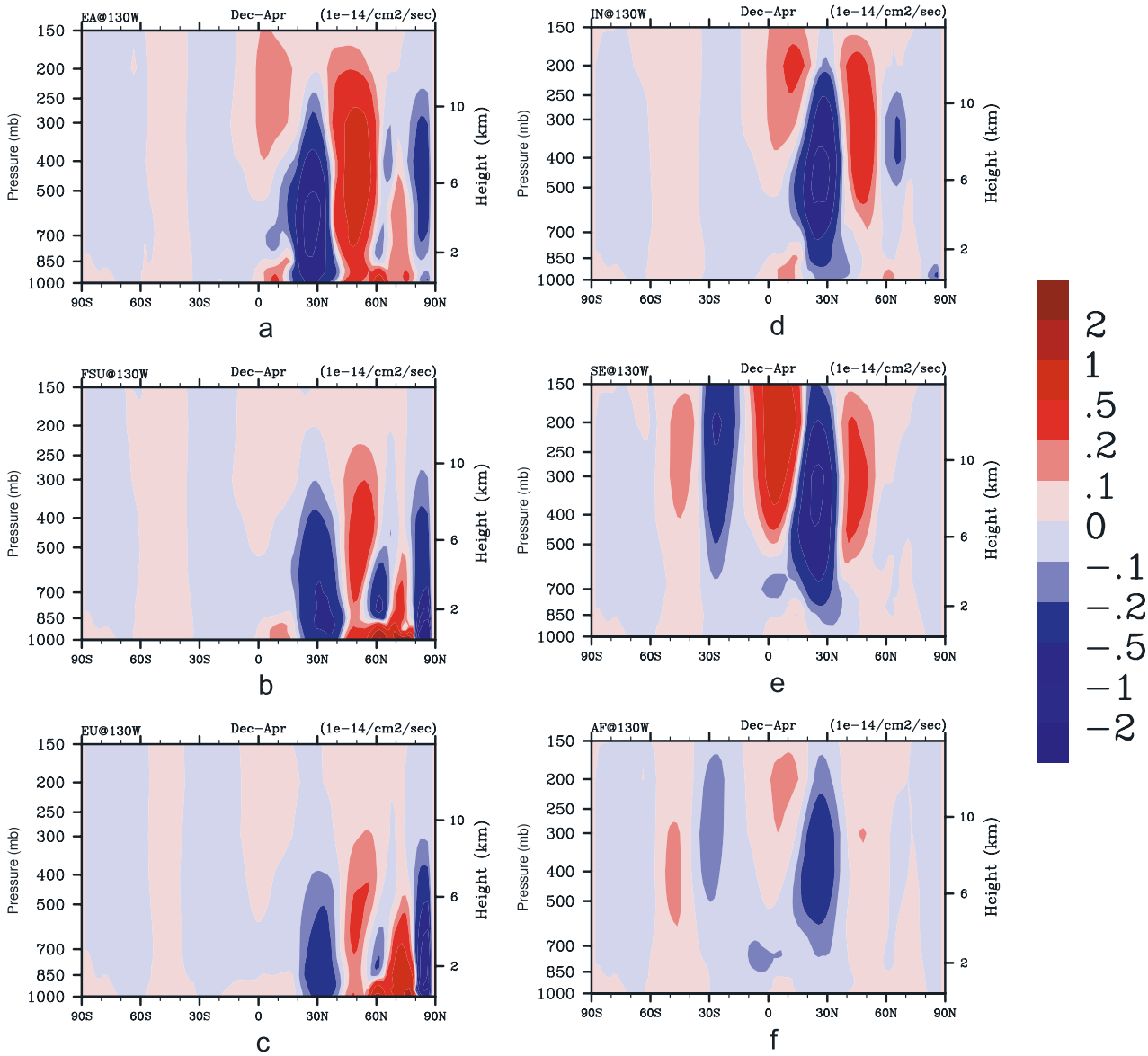

Figure 9. Regressions of monthly SOI and the anomalies of monthly transport potential flux at 130°W between December and April over the period 1991–2001 of tracers from (a) east Asia, (b) the former Soviet Union (FSU) and Middle East, (c) Europe, (d) India, (e) Southeast Asia, and (f) Africa. A positive regression indicates stronger (weaker) eastward transport during La Niña (El Niño); a negative regression indicates less (more) eastward transport during La Niña (El Niño).

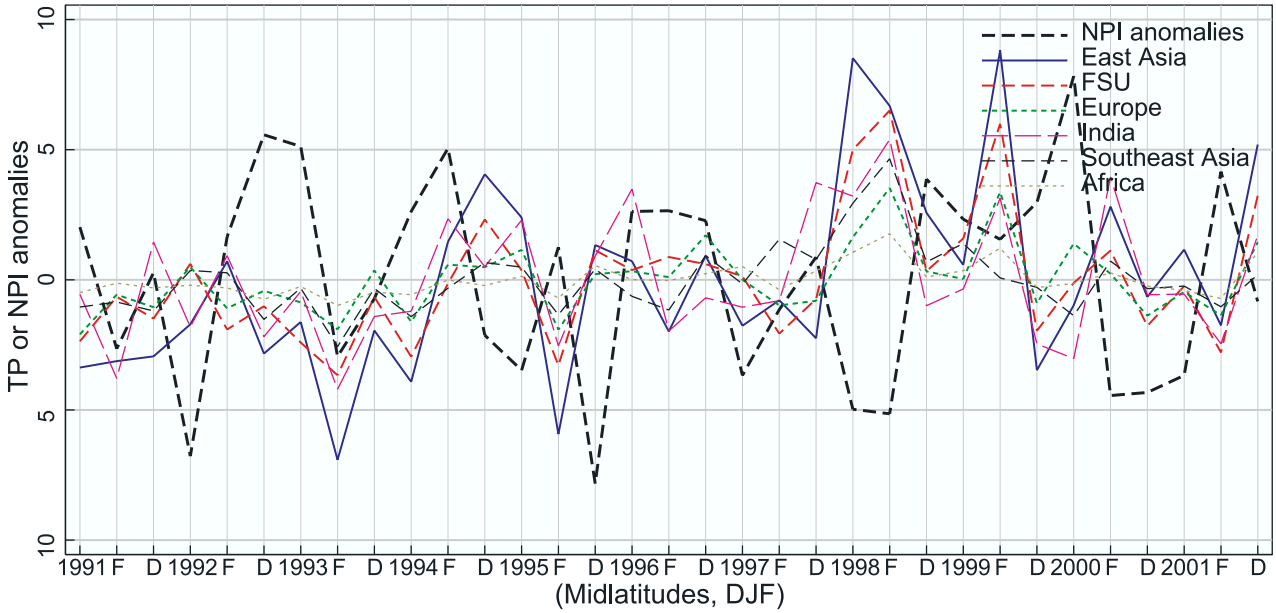

Figure 10. Time series of monthly mean anomalies of NPI and of midlatitude (30–50°N) transport potentials at 130°W in winter (DJF).

midlatitudes, missing the regions most affected by both SOI and NPI.

[32] To detect the leading meteorological component that influences the interannual variability of transport of east Asian tracer over the eastern Pacific, we define a new EPI by subtracting the area-weighted surface pressure anomalies over (20–25°N, 140–130°W) from (50–55°N, 135–125°W). These two regions were selected because of the strong correlation between the monthly midlatitude transport potential anomalies of the east Asian tracer and the monthly surface pressure anomalies seen in winter-spring at these locations (Figure 12). The EPI explains most of the interannual variability (r^2 = 0.60) in the transport of east Asian tracer over the eastern Pacific, particularly in the midlatitude regions (Figure 11c). Lower values of this index (i.e., a low pressure anomaly over the Gulf of Alaska and a high pressure anomaly over the subtropical eastern Pacific) correspond to stronger winds which increase transport of east Asian tracers to the west coast of the United States.

[33] The meteorological patterns associated with the EPI are shown in Figure 13. Low EPI values are generally associated with a deeper low over the Gulf of Alaska and a stronger westerly jet at midlatitudes over the eastern Pacific in winter. This correlation pattern persists in spring and fall, but weakens in summer.

[34] The EPI accounts for most of the interannual variability of the transport potential of the east Asian tracer across 130°W (Figure 14), with a strong anticorrelation at midlatitudes (r = −0.77) and a positive correlation at high latitudes (r = 0.64), indicating that the interannual variability is mostly driven by local meteorology over the eastern Pacific. However, there are still short periods of inconsistency, such as April 1998, when the EPI suggests no abnormal transport but relatively weak transport is observed. This suggests that meteorology elsewhere (e.g., over the east Asian continent or the western and central Pacific) can occasionally drive variations in transport.

[35] Since the interannual variability in transport is similar for most tracers, the EPI can be extended to other tracers with a similar midlatitude transport pathway. Table 4 indicates that strong correlations exist between the EPI and the transport potentials of other regional tracers (particularly FSU and European tracers) at midlatitudes. In addition, the correlations between the EPI and other indices are low (Table 5) indicating that the EPI is independent of the other indices. We have only examined the ability of the EPI to explain transpacific transport between 1991 and 2001. In the future, the EPI should be examined over a longer time period to evaluate its ability to consistently explain tracer transport across the midlatitude eastern Pacific to the United States.

7. Conclusions

[36] Our objective was to evaluate the contribution of meteorology to the interannual variability of transpacific transport. We therefore conducted a global chemical tracer model simulation of idealized tracers from nine continental regions using MOZART-2 driven with NCEP/NCAR reanalysis data from 1991 to 2001. To identify the major transport pathways, tracer fluxes (rather than tracer concentrations, which are a result of transport) are used. Midlati-

Table 3. Correlation Coefficients Between Monthly NPI Anomalies and Monthly Extratropical Transport Potential Anomalies (30°N–80°N) at 130°W for Each Season (1991–2001)

Region	DJF	MAM	JJA	SON
EA	−0.01	−0.17	−0.07	0.23
FSU	−0.03	0.24	0.11	0.43
EU	0.17	0.37	0.02	0.32
IN	−0.12	−0.56	−0.29	−0.10
SE	−0.35	−0.62	−0.42	−0.48
AF	−0.21	−0.23	−0.10	0.01

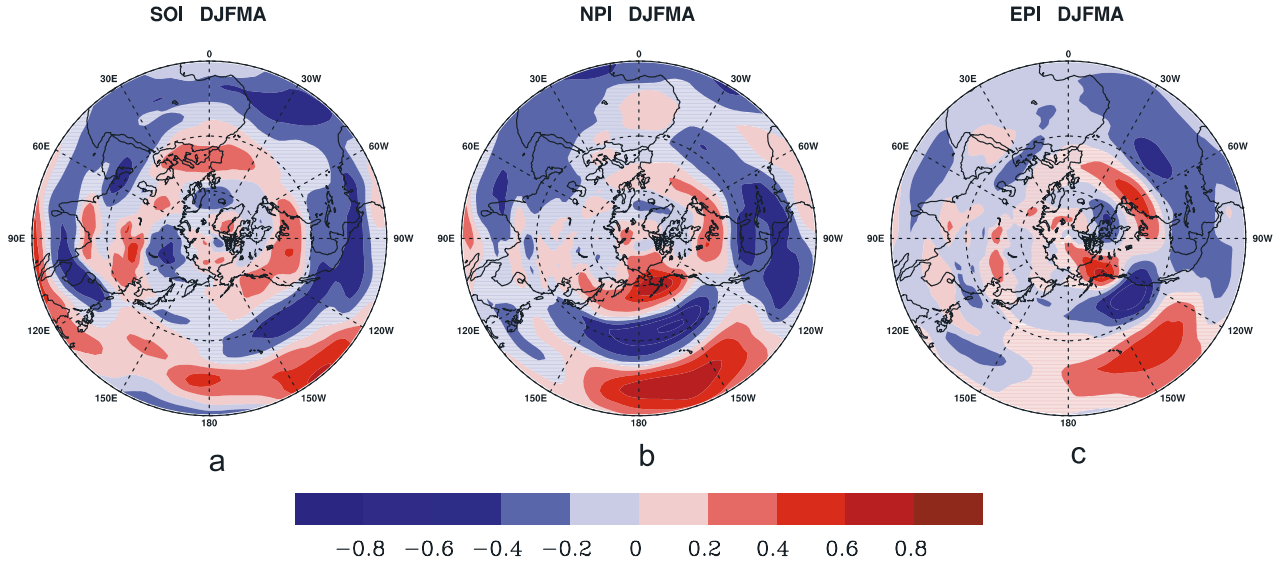

Figure 11. Horizontal distribution of correlation coefficients between the monthly mean anomalies of total column zonal flux of east Asian tracer in winter and spring (DJFMA), and the monthly mean of (a) SOI, (b) NPI anomalies, and (c) Eastern Pacific Index. (Shaded regions represent land.)

tude transport in the free troposphere is found to be the major transpacific pathway not only for east Asian emissions, but also for emissions from Europe, Africa and other Asian regions. In addition, transport across the polar region provides a secondary pathway for European and FSU tracers to reach Canada and the northeastern United States in winter and early spring.

[37] The primary transpacific transport pathways are also the most rapid, as indicated by the transport timescales. Transport of east Asian tracer to North America is more rapid than the transport of other tracers, both at the surface and in the free troposphere. However, springtime transport of the Indian tracer in the free troposphere is also rapid, requiring only 2–3 weeks on average (similar to the east Asian tracer) to cross the Pacific.

[38] We defined the "transpacific transport potential," the normalized flux across a meridional plane off the west coast of the United States (130°W), to compare the efficiency of tracer transport from Asia, Europe, and Africa across the Pacific. The transport potentials at middle and high latitudes at 130°W are generally higher than in the subtropics. The regions with the highest transport potential at high latitudes are east Asia and FSU, at midlatitudes are east Asia and India, and in the subtropics are India and southeast Asia. April is the month of strongest midlatitude transport and low interannual variability in transport determined by meteorology (especially for east Asian emissions). Thus long-term measurements over the western United States in April would reflect interannual variability in emissions and photochemistry more than other months. February is associated with both high transport and the highest levels of interannual variability. In addition, the transport potentials of FSU, east

Table 4. Correlation Coefficients Between Monthly EPI and TP Anomalies of Tracers Over the Period 1991–2001[a]

Region	Tropical Plane	Midlatitude Plane	High-Latitude Plane
EA		0.7736	−0.6388
FSU	−0.2353	0.8738	−0.4490
EU	−0.2237	0.8191	−0.4893
IN		0.5452	−0.5841
SE		0.5470	−0.6375
AF		0.6825	−0.5788

[a]Blank entries indicate no significance at the 5% level.

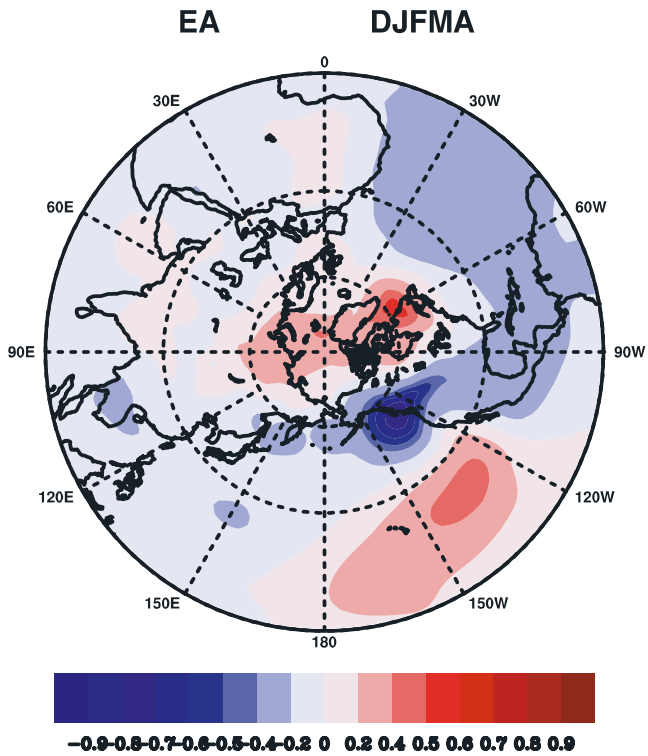

Figure 12. Horizontal distribution of correlation coefficients between monthly midlatitude transport potential anomalies of the east Asian tracer and monthly surface pressure anomalies in winter and spring (DJFMA). (Shaded regions represent land.)

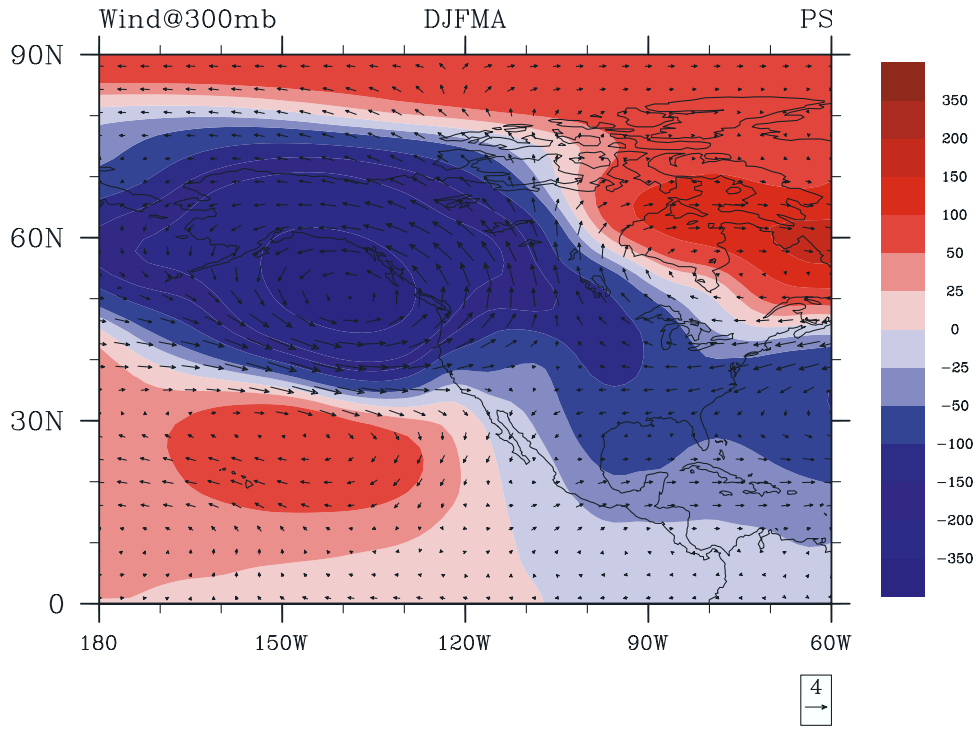

Figure 13. Horizontal distribution of regressions in DJFMA of the negative of the EPI and the monthly anomalies of (1) wind fields near 300 mb (arrows, unit: m s^{-1}) and (2) surface pressure (contours, unit: Pa).

Asian and European tracers at high latitudes in late summer and fall are also large, but with relatively low variability in transport. In the future, additional investigation of midlatitude transpacific transport in February and high-latitude transport in late summer and fall would be worthwhile.

[39] The interannual variability of transpacific transport results from large-scale variations in atmospheric circulation. Patterns of interannual variability in transpacific transport potentials, however, are similar for most tracers, indicating that the interannual variability of transpacific transport is largely driven by one dominant meteorological process. However, we find that the interannual variability in transport of the east Asian tracer is the lowest of all tracers with transport particularly stable in April. ENSO has a strong influence on the transport of the east Asian tracer in winter

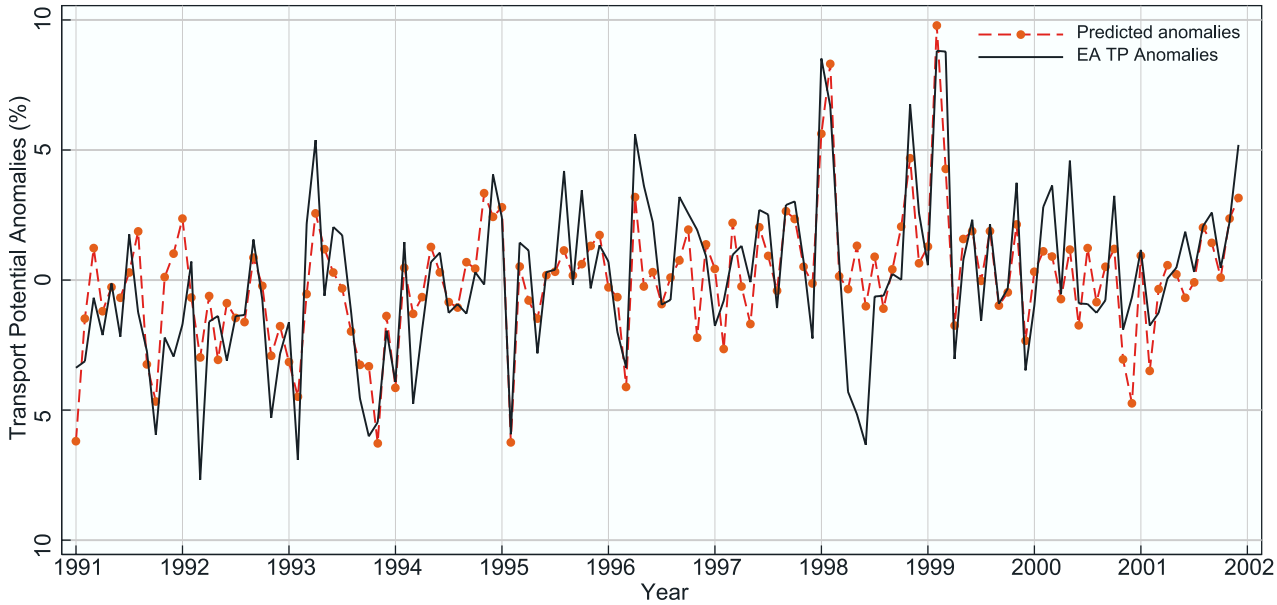

Figure 14. Time series of the monthly transport potential anomalies of the east Asian tracer across the midlatitude plane at 130°W (solid line) and its prediction by the EPI (dotted dash line).

Table 5. Correlation Coefficients of the Monthly EPI, PNA, SOI, and NPI Anomalies (1991–2001)[a]

	EPI	PNA	NPI Anomalies	SOI
EPI	1.0000			
PNA	0.1438[b]	1.0000		
NPI Anomalies	−0.2273	−0.5225	1.0000	
SOI	−0.0594[b]	−0.2634	0.2516	1.0000

[a]Excluding June and July; PNA, Pacific/North American index.
[b]Not significant at the 5% level.

over the tropical and subtropical eastern Pacific. Strong influence from El Niño is found for subtropical transport in winter, particularly for southeast Asian and African tracers ($r = -0.77$). The El Niño signal persists for subtropical transport in spring and fall, but almost disappears in summer. Extratropical transport of the east Asian tracer tends to be stronger (weaker) in the La Niña (El Niño) spring and fall. In winter and spring, El Niño (La Niña) is generally associated with a southward (northward) shift of the transport pathway, resulting in more (less) eastward transport of tracers at 30°N, but less (more) transport at 50°N. In addition, eastward transport of European and FSU tracers in the polar region is stronger during El Niño, while eastward transport of the southeast Asian tracer in the tropical upper troposphere is stronger during La Niña.

[40] The North Pacific Index influences transport over the central North Pacific, but has little influence over the eastern Pacific. The linkage between the SOI and NPI and transpacific transport potentials at middle and high latitudes, which depend on meteorological conditions over the eastern Pacific, is weak.

[41] We defined an EPI based on surface pressure gradients in the east Pacific. This index captures most of the interannual variability of the transport of the east Asian tracer over the eastern Pacific, particularly at middle and high latitudes. Generally, lower (higher) values of this index indicate stronger (weaker) eastward transport of the east Asian tracer at the west coast of the United States, but weaker (stronger) eastward transport over Alaska, the northeastern United States and the subtropical eastern Pacific. Moreover, this index can be used to estimate the midlatitude transport of other regional tracers carried in the midlatitude westerlies over the eastern Pacific.

[42] Our analysis is based on an 11-year model simulation from 1991 to 2001. The period of ENSO varies from three to seven years [*Philander and Fedorov*, 2003] and a decadal variation pattern has been observed for the Aleutian low pressure system over the North Pacific [*Trenberth and Hurrell*, 1994]. Therefore a longer period of simulation would be useful to confirm the conclusions drawn in this study.

[43] We found that ENSO influences transport in winter over the tropical and subtropical eastern Pacific, NPI influences transport over the central North Pacific and our new EPI influences transport over the eastern Pacific. Therefore in the future the ENSO, NPI and EPI indices can be used together to evaluate the transpacific transport of emissions from Asia, Europe and Africa.

[44] **Acknowledgments.** We thank the Geophysical Fluid Dynamics Laboratory for computational resources. We are pleased to acknowledge funding from a NASA New Investigator Program grant and a NASA ACMAP grant to D. Mauzerall. We thank Ants Leetmaa, Bud Moxim, Isidoro Orlanski, and George Philander for helpful discussions.

References

Bailey, R., L. A. Barrie, C. J. Halsall, P. Fellin, and D. C. G. Muir (2000), Atmospheric organochlorine pesticides in the western Canadian Arctic: Evidence of transpacific transport, *J. Geophys. Res.*, *105*(D9), 11,805–11,811.

Balkanski, Y. J., D. J. Jacob, R. Arimoto, and M. A. Kritz (1992), Distribution of Rn-222 over the North Pacific—Implications for continental influences, *J. Atmos. Chem.*, *14*(1–4), 353–374.

Berntsen, T. K., S. Karlsdottir, and D. A. Jaffe (1999), Influence of Asian emissions on the composition of air reaching the northwestern United States, *Geophys. Res. Lett.*, *26*(14), 2171–2174.

Bey, I., D. J. Jacob, J. A. Logan, and R. M. Yantosca (2001), Asian chemical outflow to the Pacific in spring: Origins, pathways, and budgets, *J. Geophys. Res.*, *106*(D19), 23,097–23,113.

Carolina Environment Program (CEP) (2004), Intercontinental transport and climatic effects of air pollution workshop presentations, Chapel Hill, N. C. (Available at http://www.cep.unc.edu/empd/projects/ICAP/2004wkshp_pres.html.)

Davis, D. D., et al. (2003), An assessment of western North Pacific ozone photochemistry based on springtime observations from NASA's PEM-West B (1994) and TRACE-P (2001) field studies, *J. Geophys. Res.*, *108*(D21), 8829, doi:10.1029/2002JD003232.

de Laat, A. T. J., J. Lelieveld, G. J. Roelofs, R. R. Dickerson, and J. M. Lobert (2001), Source analysis of carbon monoxide pollution during INDOEX 1999, *J. Geophys. Res.*, *106*(D22), 28,481–28,495.

Fiore, A. M., D. J. Jacob, I. Bey, R. M. Yantosca, B. D. Field, A. C. Fusco, and J. G. Wilkinson (2002), Background ozone over the United States in summer: Origin, trend, and contribution to pollution episodes, *J. Geophys. Res.*, *107*(D15), 4275, doi:10.1029/2001JD000982.

Hack, J. J. (1994), Parameterization of moist convection in the National Center for Atmospheric Research community climate model (CCM2), *J. Geophys. Res.*, *99*, 5541–5568.

Heald, C. L., et al. (2003), Asian outflow and trans-Pacific transport of carbon monoxide and ozone pollution: An integrated satellite, aircraft, and model perspective, *J. Geophys. Res.*, *108*(D24), 4804, doi:10.1029/2003JD003507.

Hess, P. G., and T. Vukicevic (2003), Intercontinental transport, chemical transformations, and baroclinic systems, *J. Geophys. Res.*, *108*(D12), 4354, doi:10.1029/2002JD002798.

Horowitz, L. W., et al. (2003), A global simulation of tropospheric ozone and related tracers: Description and evaluation of MOZART, version 2, *J. Geophys. Res.*, *108*(D24), 4784, doi:10.1029/2002JD002853.

Jacob, D. J., J. A. Logan, and P. P. Murti (1999), Effect of rising Asian emissions on surface ozone in the United States, *Geophys. Res. Lett.*, *26*(14), 2175–2178.

Jacob, D. J., J. H. Crawford, M. M. Kleb, V. S. Connors, R. J. Bendura, J. L. Raper, G. W. Sachse, J. C. Gille, L. Emmons, and C. L. Heald (2003), Transport and Chemical Evolution over the Pacific (TRACE-P) aircraft mission: Design, execution, and first results, *J. Geophys. Res.*, *108*(D20), 9000, doi:10.1029/2002JD003276.

Jaffe, D., et al. (1999), Transport of Asian air pollution to North America, *Geophys. Res. Lett.*, *26*(6), 711–714.

Jaffe, D., I. McKendry, T. Anderson, and H. Price (2003), Six "new" episodes of trans-Pacific transport of air pollutants, *Atmos. Environ.*, *37*(3), 391–404.

Jaffe, D., I. Bertschi, L. Jaeglé, P. Novelli, J. S. Reid, H. Tanimoto, R. Vingarzan, and D. L. Westphal (2004), Long-range transport of Siberian biomass burning emissions and impact on surface ozone in western North America, *Geophys. Res. Lett.*, *31*, L16106, doi:10.1029/2004GL020093.

Kalnay, E., et al. (1996), The NCEP/NCAR 40-year reanalysis project, *Bull. Am. Meteorol. Soc.*, *77*(3), 437–471.

Lamarque, J., and P. G. Hess (2004), Arctic Oscillation modulation of the Northern Hemisphere spring tropospheric ozone, *Geophys. Res. Lett.*, *31*, L06127, doi:10.1029/2003GL019116.

Li, Q. B., et al. (2001), A tropospheric ozone maximum over the Middle East, *Geophys. Res. Lett.*, *28*(17), 3235–3238.

Lin, C. Y. C., D. J. Jacob, J. W. Munger, and A. M. Fiore (2000), Increasing background ozone in surface air over the United States, *Geophys. Res. Lett.*, *27*(21), 3465–3468.

Lin, S. J., and R. B. Rood (1996), Multidimensional flux-form semi-Lagrangian transport schemes, *Mon. Weather Rev.*, *124*(9), 2046–2070.

Liu, H., D. J. Jacob, I. Bey, R. M. Yantosca, B. N. Duncan, and G. W. Sachse (2003), Transport pathways for Asian pollution outflow over the Pacific: Interannual and seasonal variations, *J. Geophys. Res.*, *108*(D20), 8786, doi:10.1029/2002JD003102.

Mauzerall, D. L., J. A. Logan, D. J. Jacob, B. E. Anderson, D. R. Blake, J. D. Bradshaw, B. Heikes, G. W. Sachse, H. Singh, and B. Talbot (1998), Photochemistry in biomass burning plumes and implications for tropospheric ozone over the tropical South Atlantic, *J. Geophys. Res.*, *103*(D7), 8401–8423.

Mauzerall, D. L., D. Narita, H. Akimoto, L. Horowitz, S. Walters, D. A. Hauglustaine, and G. Brasseur (2000), Seasonal characteristics of tropospheric ozone production and mixing ratios over east Asia: A global three-dimensional chemical transport model analysis, *J. Geophys. Res.*, *105*(D14), 17,895–17,910.

McKeen, S. A., and S. C. Liu (1993), Hydrocarbon ratios and photochemical history of air masses, *Geophys. Res. Lett.*, *20*(21), 2363–2366.

McKeen, S. A., S. C. Liu, E. Y. Hsie, X. Lin, J. D. Bradshaw, S. Smyth, G. L. Gregory, and D. R. Blake (1996), Hydrocarbon ratios during PEM-WEST A: A model perspective, *J. Geophys. Res.*, *101*(D1), 2087–2109.

Orlanski, I. (2003), Bifurcation in eddy life cycles: Implications for storm track variability, *J. Atmos. Sci.*, *60*(8), 993–1023.

Philander, S. G., and A. Fedorov (2003), Is El Nino sporadic or cyclic?, *Annu. Rev. Earth Planet. Sci.*, *31*, 579–594.

Stohl, A., S. Eckhardt, C. Forster, P. James, and N. Spichtinger (2002), On the pathways and timescales of intercontinental air pollution transport, *J. Geophys. Res.*, *107*(D23), 4684, doi:10.1029/2001JD001396.

Trenberth, K. E. (1984), Signal versus noise in the Southern Oscillation, *Mon. Weather Rev.*, *112*(2), 326–332.

Trenberth, K. E., and J. W. Hurrell (1994), Decadal atmosphere-ocean variations in the Pacific, *Clim. Dyn.*, *9*(6), 303–319.

Verver, G. H. L., D. R. Sikka, J. M. Lobert, G. Stossmeister, and M. Zachariasse (2001), Overview of the meteorological conditions and atmospheric transport processes during INDOEX 1999, *J. Geophys. Res.*, *106*(D22), 28,399–28,413.

Wild, O., and H. Akimoto (2001), Intercontinental transport of ozone and its precursors in a three-dimensional global CTM, *J. Geophys. Res.*, *106*(D21), 27,729–27,744.

Wilkening, K. E. (2001), Trans-Pacific air pollution: Scientific evidence and political implications, *Water Air Soil Pollut.*, *130*(1–4), 1825–1830.

Yienger, J. J., M. Galanter, T. A. Holloway, M. J. Phadnis, S. K. Guttikunda, G. R. Carmichael, W. J. Moxim, and H. Levy (2000), The episodic nature of air pollution transport from Asia to North America, *J. Geophys. Res.*, *105*(D22), 26,931–26,945.

Zhang, G. J., and N. A. Mcfarlane (1995), Sensitivity of climate simulations to the parameterization of cumulus convection in the Canadian Climate Center general circulation model, *Atmos. Ocean*, *33*(3), 407–446.

Zhang, Y., K. R. Sperber, and J. S. Boyle (1997), Climatology and interannual variation of the East Asian winter monsoon: Results from the 1979–95 NCEP/NCAR reanalysis, *Mon. Weather Rev.*, *125*(10), 2605–2619.

L. W. Horowitz, Geophysical Fluid Dynamics Laboratory, Princeton, NJ 08542, USA.

J. Liu and D. L. Mauzerall, Woodrow Wilson School of Public and International Affairs, Princeton University, Princeton, NJ 08544, USA. (mauzeral@princeton.edu)